JOURNAL OF VIROLOGY, June 2003, p. 6574–6579 Vol. 77, No. 11
0022-538X/03/$08.00+0 DOI: 10.1128/JVI.77.11.6574–6579.2003

Viral Internal Ribosome Entry Site Structures Segregate into Two Distinct Morphologies

Lucy P. Beales,[1]* Andreas Holzenburg,[2] and David J. Rowlands[1]

Division of Microbiology, School of Biochemistry and Molecular Biology, University of Leeds, Leeds LS2 9JT, United Kingdom,[1] and Electron Microscopy Centre and Department of Biology, Texas A&M University, College Station, Texas 77843[2]

Received 4 September 2002/Accepted 6 March 2003

An increasing number of viruses have been shown to initiate protein synthesis by a cap-independent mechanism involving internal ribosome entry sites (IRESs). Predictions of the folding patterns of these RNA motifs have been based primarily on sequence and biochemical analyses. Biophysical confirmation of the models has been achieved only for the IRES of hepatitis C virus (HCV), which adopts an open structure consisting of two major stems. We have conducted an extensive comparison of flavivirus and picornavirus IRES elements by negative stain transmission electron microscopy. All of the flavivirus IRESs we examined (those of GB virus-B, GB virus-C, and classical swine fever virus) fold to give a structure similar to that of the HCV IRES, as does an IRES recently found on mRNA encoded by human herpesvirus 8. The larger picornavirus IRESs (those of foot-and-mouth disease virus, rhinovirus, encephalomyocarditis virus, and hepatitis A virus) are morphologically similar, comprising a backbone with two protruding stems, and distinct from the flavivirus IRESs.

For many RNA virus genomes, translation is initiated by a process different from the usual eukaryotic cap-dependent mechanism. These viruses possess long 5′ untranslated regions (UTRs) that are well conserved, highly structured, and include internal ribosome entry sites (IRESs) (25). Conversely, the great majority of eukaryotic mRNAs have an mGpppX cap structure at the 5′ end that interacts with a subunit (eIF4E) of the heterotrimeric initiation factor eIF4F. The eIF4F complex, which also contains the bridging protein eIF4G and helicase eIF4A, facilitates the docking of the 43S complex, comprising eIF3 and the 40S ribosomal subunit charged with eIF2-GTP-Met-tRNA, via interaction of eIF3 with eIF4G. With the aid of additional initiation factors, the small ribosomal subunit scans the mRNA from the 5′ UTR until the initiation codon is reached. The 60S ribosomal subunit then binds, initiation factors are released, and translation begins.

Cap-independent initiation of translation was first described for picornaviruses (23). The uncapped 5′ UTR of each of the picornavirus RNA genomes contains an ordered structure of 400 to 450 nucleotides (nt) that allows assembly of the translational machinery at a position close to or directly at the initiation codon. This interaction is independent of the nature of the extreme 5′ end of the RNA as it does not require a cap structure and occurs when the sequence is inserted between the cistrons of an artificially constructed bicistronic mRNA. Most of the picornaviruses express a protease that specifically cleaves eIF4G, such that the portion of the protein that interacts with eIF4E (cap-binding protein) is removed from the domains of eIF4G that interact with the 43S ternary complex (17). Thus, upon infection with these viruses, host protein synthesis is blocked and the viral genome is translated without competition from cellular mRNAs for the required host components. The cleaved eIF4G (p100) is able to interact with the majority of picornavirus IRESs in the absence of the eIF4E-binding domain (6, 22, 24). This interaction may require noncanonical host factors.

The picornavirus IRESs have been classified into three types based on their primary and secondary structures (13). Enteroviruses and rhinoviruses have type I IRESs, whereas aphthoviruses and cardioviruses contain type II IRESs. These IRES groups differ in host protein requirements as well as in the positions of the initiation codons with regard to the entry sites. The IRES of hepatitis A virus (HAV) is distinct from that of other picornaviruses and makes up a group (type III) on its own. Infection with this virus does not result in cleavage of eIF4G, and translation from its IRES requires intact eIF4G as well as the presence of eIF4E (1, 5).

Following the initial characterization of picornavirus IRESs, other RNA viruses were shown to initiate translation internally. These include members of the family *Flaviviridae*, the pestiviruses (e.g., bovine viral diarrhea virus [9] and classical swine fever virus [CSFV] [29]) and hepaciviruses (e.g., hepatitis C virus [HCV] [31]), which contain IRESs located largely within the 5′ UTRs but also involving sequences within the start of the coding regions (27). IRESs have also been identified within the coding regions of retroviruses (Moloney murine leukemia virus [32], simian immunodeficiency virus [21], and human immunodeficiency virus [8]), where they mediate translation of alternative open reading frames, and in cricket paralysis virus (33). Subsequently, the DNA virus associated with Kaposi's syndrome, human herpesvirus 8 (HHV8), has been shown to translate the FLICE inhibitory protein, FLIP, from an IRES situated within the v-cyclin coding region and extending into the FLIP gene (3, 11, 19).

The secondary structures of the IRESs of picornaviruses, pestiviruses, and hepaciviruses have been mapped by using a combination of biochemical and phylogenetic analyses. Re-

* Corresponding author. Mailing address: Division of Microbiology, School of Biochemistry and Molecular Biology, University of Leeds, Old Medical School, Thoresby Place, Leeds LS2 9JT, United Kingdom. Phone: 44-113-343 5579. Fax: 44-113-343 5638. E-mail: l.p.beales@bmb.leeds.ac.uk.

cently, the proposed structural model of the HCV IRES has been confirmed and refined by using negative stain transmission electron microscopy (TEM) (2), cryo-electron microscopy (cryo-EM) (30), nuclear magnetic resonance (NMR) (16, 20), and X-ray scattering (14). However, such techniques have not been applied extensively to the characterization of the larger IRESs. We have developed a negative staining technique that allows imaging of large RNA structures by TEM, and this has enabled us to visualize and orientate the HCV IRES (2). This IRES forms an extended structure consisting of two major stems of 10 and 18 nm, formed by domains II and III, respectively (see Fig. 3a). A small spur of ~2 nm is formed by the pseudoknot structure involving domains IIIf and IV. The images obtained in that study correlate well with a cryo-EM model of the HCV IRES bound to the 40S ribosomal subunit (30). Together, these results suggest that there is little alteration of the overall architecture of the HCV IRES upon binding to the 40S ribosomal subunit other than the loss of flexibility between domains II and III. The large size of virus IRESs together with the flexibility between stems makes it difficult to utilize NMR and X-ray crystallography to obtain high-resolution data. However, we have used TEM to visualize and compare the overall architecture of the HCV IRES with that of other IRESs of flaviviral origin and with those of the different types of picornavirus IRESs. We have also compared the morphological appearances of these IRESs from RNA viruses with that of a recently described RNA sequence with IRES properties that lies within a bicistronic mRNA encoded by the DNA virus HHV8.

The predicted secondary folding structures of the IRESs in this study are shown in Fig. 1. The models were taken from the literature, as referenced in the figure legend, and were derived from a combination of RNA folding predictions, phylogenetic analyses, and direct biochemical studies. The different RNA sequences were transcribed in vitro from the following constructs. The GB virus-B (GBV-B; nt 1 to 459) and CSFV (nt 1 to 386) IRES sequences were amplified by PCR from constructs provided by S. Lemon (University of Texas Medical Branch, Galveston), and the amplified sequences were cloned into pCR Blunt (Invitrogen). A construct containing the GBV-C IRES sequence (nt 66 to 639) was kindly donated by J. Stapleton (University of Iowa, Iowa City). The HHV8 IRES (255 nt immediately upstream of the v-FLIP coding region) was amplified from construct pBKLCK (pBKCMV vector [Promega] containing HHV8 latent nuclear antigen, v-cylin, and v-FLIP genes), donated by P. Kellam (Wohl Virus Institute, University College, London, United Kingdom), and cloned into pCR Blunt (Invitrogen). HAV HM175/18f.1 (nt 225 to 746) (18) and human rhinovirus 14 (HRV 14; nt 1 to 628) IRESs were amplified by PCR with forward primers containing the T7 RNA polymerase promoter sequence and appropriate restriction endonuclease sites and cloned into a Bluescript SK(+) vector (Stratagene) by using *Xho*I and *Eco*RI restriction sites. The IRES RNAs were transcribed by using 5 μg of T7 RNA polymerase in a 100-μl reaction mix containing 10 μg of linearized plasmid, 80 mM HEPES-KOH (pH 7.5), 24 mM $MgCl_2$, 2 mM spermidine, 40 mM dithiothreitol, 7.5 mM (each) ribonucleotide triphosphates, 0.5 U of inorganic pyrophosphatase, and 4 U of RNase inhibitor. The transcription reactions mixtures were incubated overnight at 37°C, after which the templates were digested with 10 U of RNase-free DNase (Promega) for 15 min at 37°C. Transcribed RNA was purified by phenol chloroform extraction followed by ethanol precipitation and washing. The resuspended RNA was further purified by using a Nanosep 10K filter (Flowgen). The integrity of the purified transcripts was determined by electrophoresis on a 6% polyacrylamide–7 M urea–Tris-borate-EDTA gel (Fig. 2). To ensure correct folding of the IRESs, magnesium chloride was added to the RNA to a concentration of 5 mM and the solution was heated to 65°C for 1 min followed by cooling to room temperature for 30 min.

The RNAs were mounted on grids for EM as previously described (2). Briefly, the RNA was diluted to 2.5 μg ml^{-1} (approximately 10^{14} molecules ml^{-1}), adsorbed onto a carbon film for 30 s, washed in distilled water for 10 s, and negatively stained by using a 2% (wt/vol) aqueous solution of uranyl acetate for 1 min. Specimens were then mounted onto gold-plated copper grids (400 mesh) and blotted dry. Micrographs were recorded on Agfa Scientia 23D56 electron image sheet films at calibrated magnifications with a Philips CM10 transmission electron microscope operated at 100 kV. Each set of images in Fig. 3 and 4 shows examples of IRES structures of which at least 100 such images were seen.

As a negative control, a random 340-nt RNA fragment was transcribed from the parental Bluescript SK(+) vector after digestion with restriction enzyme *Pvu*I by using T7 RNA polymerase. When the control was examined by the above-described negative stain EM method, no RNA structures were seen, even at concentrations 10-fold higher than those used for the IRES RNA transcripts, indicating that tertiary structures of the complexity of the IRES elements visualized in this study are not formed by this random RNA fragment.

Flavivirus IRESs. The HCV IRES was previously shown by TEM to comprise two stems, one of 18 nm (stem a, equivalent to domain II) and one of 10 nm (stem b, equivalent to domain III), and a small spur of approximately 2 nm (stem c, equivalent to domain IV) (2). Little interaction between individual domains of the HCV IRES is required for the formation of this structure. A transcript representing nt 119 to 156 of the HCV 5′ UTR was examined to determine whether domain III of HCV can form independently of domain II, as suggested by X-ray scattering and NMR studies (15, 30). The images obtained (Fig. 3b) indicate the formation of a long stem resembling domain III (18 nm) and a short spur, which most likely corresponds to the pseudoknot region. While this truncated IRES is not capable of driving translation initiation, it does associate with the 40S ribosomal subunit (30). The correct folding of domains III and IV in the absence of the remainder of the 5′ UTR is likely to be necessary for this interaction. The precise role of domain II in HCV IRES-driven translation has yet to be established.

Related viruses within the *Flaviviridae* family are predicted to have secondary structures broadly similar to that of HCV. To determine whether these predicted structural similarities are observable in the folded RNA, we compared images of the HCV IRES with those of GBV-B (Fig. 3c) and GBV-C (Fig. 3e) IRESs and with images of the IRES of the more distantly related pestivirus CSFV (Fig. 3d). In these negative stain images, the RNA structures appear unstained on a darkly stained background. The GBV-B IRES is very similar to the HCV

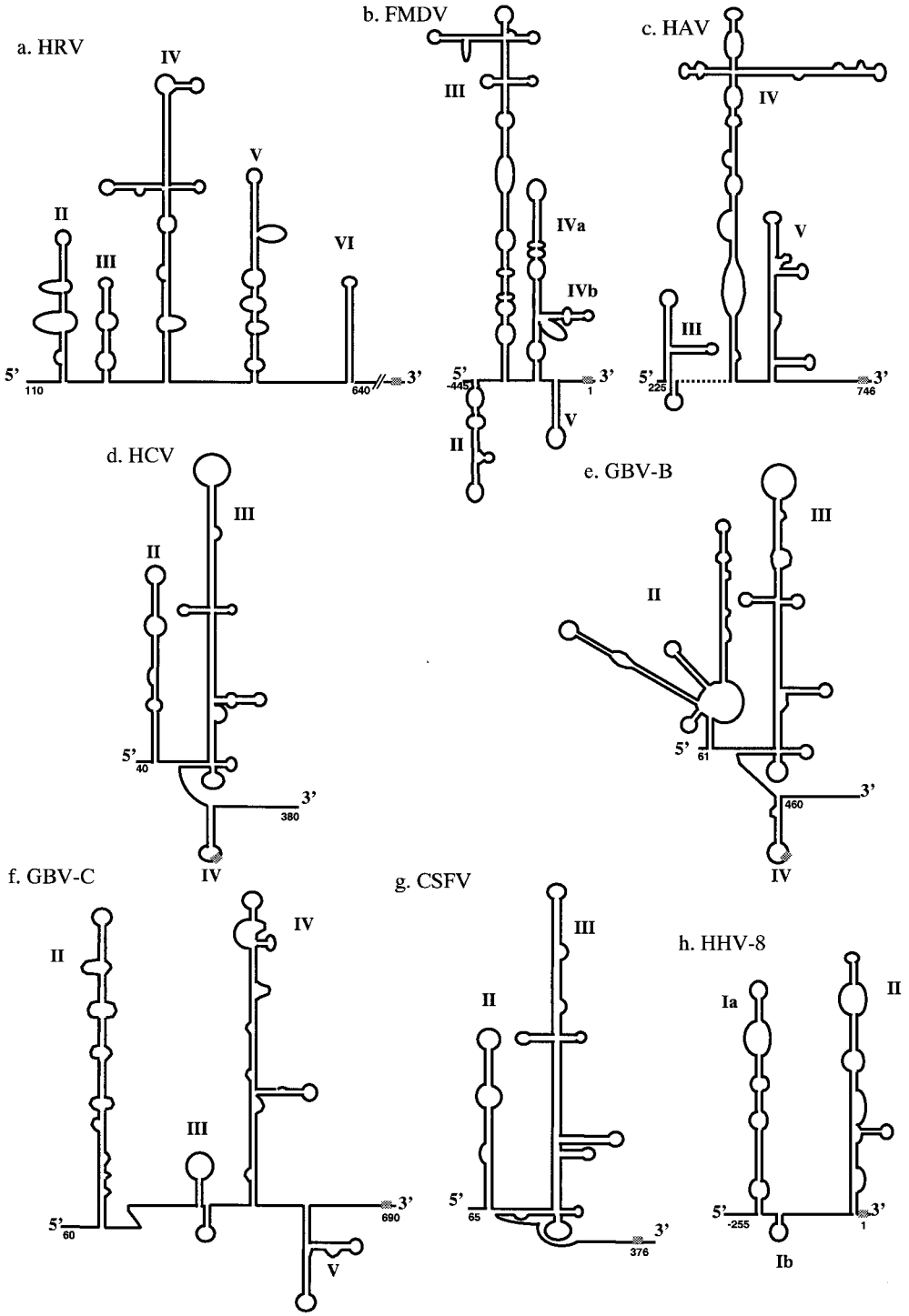

FIG. 1. Proposed secondary structures of virus IRES elements from (a) HRV (type I picornavirus IRES) (4), (b) FMDV (type II picornavirus IRES) (24), (c) HAV (type III picornavirus IRES) (7), (d) HCV (12), (e) GBV-B (28), (f) GBV-C (28), (g) CSFV (10), and (h) HHV8 (3). The numbering of nucleotides on FMDV (b) and HHV8 (h) models is from the initiation codon. In all other models, numbering is from the 5′ end of the corresponding viral genome.

IRES, comprising two stems of 18 to 20 nm (stem a) and ~10 nm (stem b). However, no small spurs were detected in these molecules. The GBV-C IRES also consists of two stems, but the molecules differ from those of HCV and GBV-B IRESs in that the stems are of similar lengths (18 nm) and there appears to be more flexibility within each stem. The CSFV IRES is also very similar to the HCV IRES, being composed of two major stems of 18 nm (stem a) and 8 nm (stem b).

Thus, all of the flavivirus IRESs examined appear as forked structures with two long stems flexibly linked at their bases by

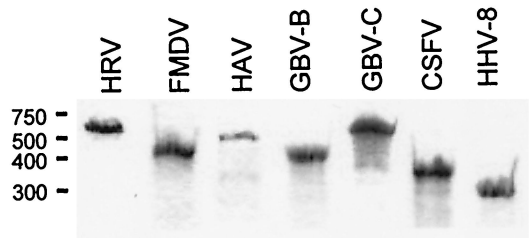

FIG. 2. Polyacrylamide gel analysis of transcribed IRES RNAs. The electrophoresed RNA was visualized by immersing the gel in 0.025% methylene blue for 1 h followed by destaining in several changes of tap water.

a domain that frequently contains a pseudoknot. A small spur domain, which may be formed by the predicted pseudoknot, can sometimes be seen at this junction. It is likely that the longer stem, stem a, corresponds to domain III in the predicted models of GBV-B and CSFV IRES elements. The predicted structure of the GBV-B IRES differs from that of the others in that domain II is thought to comprise three distinct stem-loops. However, these additional stems are not apparent in the EM images of the GBV-B IRES and it is possible that they are stacked to form stem b and therefore not distinguishable as individual domains.

The predicted model of the GBV-C IRES structure differs from that of the HCV IRES in that domain II is larger, forming a single stem-loop similar in length to domain III, and a pseudoknot structure may form between the domains. This model is supported by our EM images that show double-stemmed structures with arms of similar lengths.

HHV8 IRES. The flavivirus and picornavirus IRESs are all located within the 5′ UTRs of their respective genomes, and these elements appear to be structurally conserved within the viral families. HHV8 is the only DNA virus that has been shown to encode an IRES, which is located in the intercistronic region of a bicistronic mRNA. Again, EM revealed structures of defined morphologies which bore a remarkable similarity to the HCV IRES, although they were of smaller size (Fig. 3f). The structures comprised two stems measuring 12 nm (stem a) and 5 nm (stem b), with a flexible hinge region between. The longer of the two stems may relate to domain II in the predicted structure (Fig. 1h). This IRES is the smallest to be analyzed by EM, and its small size and simplicity may reflect the fact that the RNA on which this structure resides is used only for translation and not replication.

Picornavirus IRES types. The picornavirus IRESs are significantly larger than those of the flaviviruses, typically comprising 450 nt. In an earlier study we showed that the type II IRES of foot-and-mouth disease virus (FMDV) forms an f-shaped structure with a large backbone decorated by two side stems (2) (Fig. 4a). Identification of known polypyrimidine tract binding protein binding domains by immunogold labeling and negative stain EM allowed us to predict the tertiary interactions between domains. In the proposed model, domain III forms the backbone of the structure (stem a-b) and stem c, with domain II at the base of stem a-b and domain IV rotated and stacked on domain III to form the protruding stem d. This model is in agreement with the results of biochemical analysis of interactions between individual domains of the FMDV

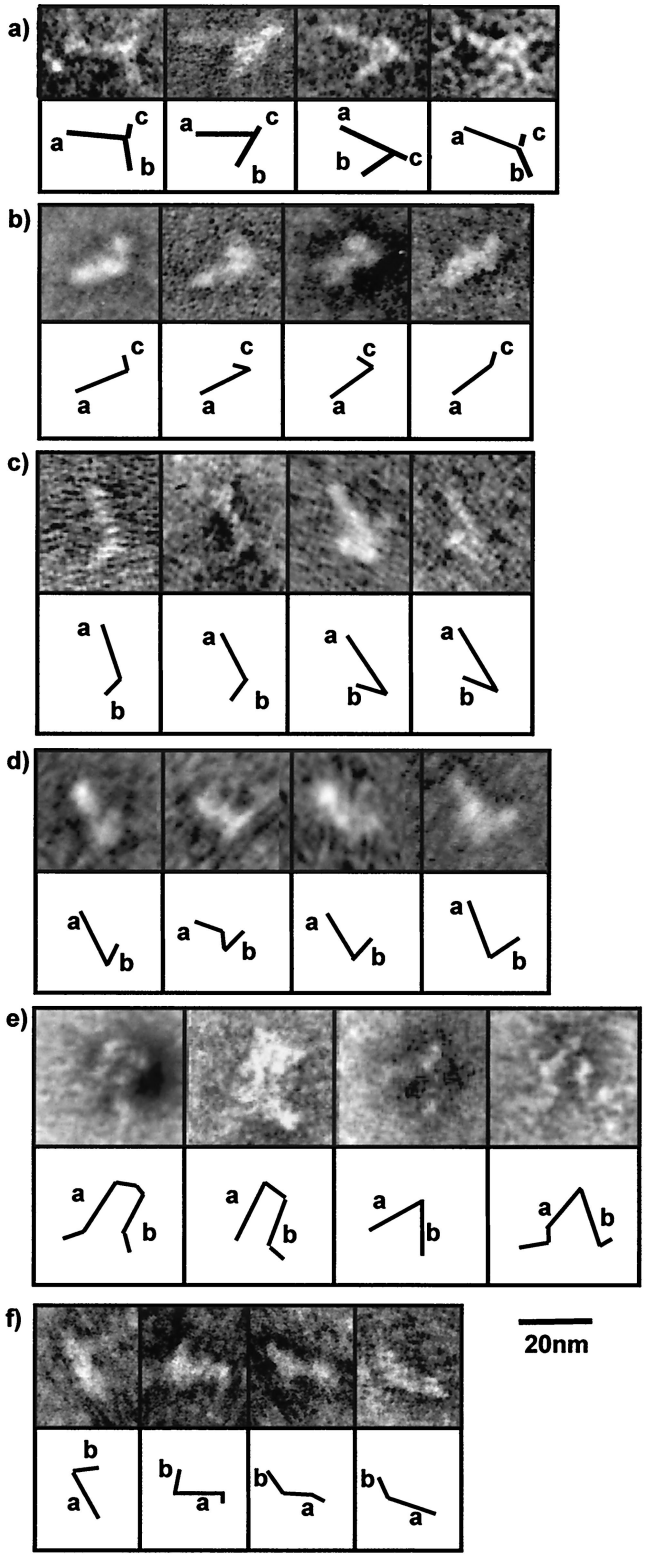

FIG. 3. Representative negative stain TEM images of flavivirus-like IRES transcripts, with diagrammatic depictions of the structures noted. (a) HCV. (b) HCV 5′ UTR nt 119 to 156 (domains III and IV). (c) GBV-B. (d) CSFV. (e) GBV-C. (f) HHV8.

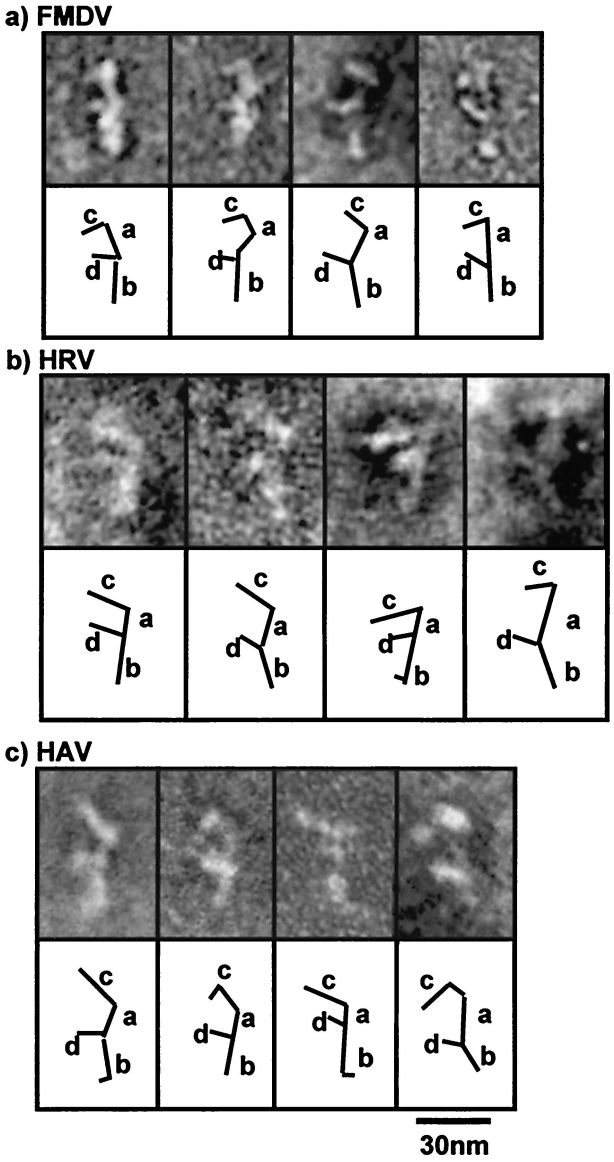

FIG. 4. Representative negative stain TEM images of picornavirus IRES transcripts, with diagrammatic depictions of the structures noted. (a) Type II. (b) Type I. (c) Type III.

IRES (26), which show that domains IV and V interact strongly with domain III but not with domain II.

The overall structure of the type I, HRV IRES element closely resembles that of the FMDV IRES, consisting of a long stem (36 to 48 nm) and two protruding stems (stems c and d) (Fig. 4b). However, there are differences in the relative lengths of stems c and d. While stem c consistently measures ~8 nm, stem d has a more variable length of 10 to 20 nm. There is also more flexibility in the base of stem a-b of the HRV IRES than in that of the FMDV IRES. While it is conceivable that the backbone stem a-b involves the largest domain (IV), the differences in predicted models for the HRV and FMDV IRES elements make it difficult to speculate on the identities of the other stems and the tertiary interactions involved. There appears to be more flexibility throughout the HRV IRES than was seen in the other picornavirus IRESs studied. This is particularly noticeable in stem c and the upper portion of stem a-b.

The overall appearance of the HAV IRES also resembles that of the FMDV IRES (Fig. 4c). The long stem (stem a-b) measures approximately ~30 nm and, again, is flexible at the base. The protruding stems have consistent lengths of ~19 nm (stem c) and ~7 nm (stem d); however, there does appear to be a little flexibility in stem d. The type III, HAV IRES has a proposed secondary structure similar to that of the FMDV IRES, and it is possible that the tertiary structure of this IRES is similarly constructed. As predicted for the FMDV IRES, stem a-b may be formed by domains IV and III, with the protruding stems c and d formed by the tops of domains IV and V, respectively. There appears to be some flexibility in the base of stem a-b of the HAV IRES, which may be due to the small stem-loop structure located between domains III and IV.

This study shows that the overall tertiary structures of IRES elements are generally similar within virus families in spite of there being very little sequence conservation. However, the ways in which these IRES elements are assembled may vary greatly, and we are addressing this uncertainty via the analysis by TEM of IRESs from which defined domains have been deleted. Conservation of tertiary structure appears to correlate with the requirements for noncanonical host protein factors during initiation of translation, the more elaborate picornavirus IRESs interacting with several more host factors than their flavivirus counterparts. Based on its small size and similarity to the flavivirus IRESs, it is tempting to speculate that the HHV8 IRES requires little in the way of host factors for efficient initiation of translation.

We thank S. Lemon (University of Texas, Galveston), J. Stapleton (University of Iowa, Iowa City), R. Jackson (University of Cambridge, Cambridge, United Kingdom), and P. Kellam (University College, London, United Kingdom) for the kind provision of IRES constructs and A. Hick for EM technical support.

This work was funded by BBSRC project grant number 24/C13923.

REFERENCES

1. **Ali, I. K., L. McKendrick, S. J. Morley, and R. J. Jackson.** 2001. Activity of the hepatitis A virus IRES requires association between the cap-binding translation initiation factor (eIF4E) and eIF4G. J. Virol. **75:**7854–7863.
2. **Beales, L. P., D. J. Rowlands, and A. Holzenburg.** 2001. The internal ribosome entry site (IRES) of hepatitis C virus visualized by electron microscopy. RNA **7:**661–670.
3. **Bieleski, L., and S. J. Talbot.** 2001. Kaposi's sarcoma-associated herpesvirus vCyclin open reading frame contains an internal ribosome entry site. J. Virol. **75:**1864–1869.
4. **Borman, A., and R. J. Jackson.** 1992. Initiation of translation of human rhinovirus RNA: mapping the internal ribosome entry site. Virology **188:** 685–696.
5. **Borman, A. M., and K. M. Kean.** 1997. Intact eukaryotic initiation factor 4G is required for hepatitis A virus internal initiation of translation. Virology **237:**129–136.
6. **Borman, A. M., R. Kirchweger, E. Ziegler, R. E. Rhoads, T. Skern, and K. M. Kean.** 1997. eIF4G and its proteolytic cleavage products: effect on initiation of protein synthesis from capped, uncapped, and IRES-containing mRNAs. RNA **3:**186–196.
7. **Brown, E. A., S. P. Day, R. W. Jansen, and S. M. Lemon.** 1991. The 5′ nontranslated region of hepatitis A virus RNA: secondary structure and elements required for translation in vitro. J. Virol. **65:**5828–5838.
8. **Buck, C. B., X. Shen, M. A. Egan, T. C. Pierson, C. M. Walker, and R. F. Siliciano.** 2001. The human immunodeficiency virus type 1 *gag* gene encodes an internal ribosome entry site. J. Virol. **75:**181–191.
9. **Chon, S. K., D. R. Perez, and R. O. Donis.** 1998. Genetic analysis of the internal ribosome entry segment of bovine viral diarrhea virus. Virology **251:**370–382.
10. **Fletcher, S. P., and R. J. Jackson.** 2002. Pestivirus internal ribosome entry

site (IRES) structure and function: elements in the 5′ untranslated region important for IRES function. J. Virol. **76:**5024–5033.
11. **Grundhoff, A., and D. Ganem.** 2001. Mechanisms governing expression of the v-FLIP gene of Kaposi's sarcoma-associated herpesvirus. J. Virol. **75:** 1857–1863.
12. **Honda, M., M. R. Beard, L. H. Ping, and S. M. Lemon.** 1999. A phylogenetically conserved stem-loop structure at the 5′ border of the internal ribosome entry site of hepatitis C virus is required for cap-independent viral translation. J. Virol. **73:**1165–1174.
13. **Jackson, R. J., M. T. Howell, and A. Kaminski.** 1990. The novel mechanism of initiation of picornavirus RNA translation. Trends Biochem. Sci. **15:**477–483.
14. **Kieft, J. S., K. Zhou, R. Jubin, M. G. Murray, J. Y. Lau, and J. A. Doudna.** 1999. The hepatitis C virus internal ribosome entry site adopts an ion-dependent tertiary fold. J. Mol. Biol. **292:**513–529.
15. **Kim, I., P. J. Lukavsky, and J. D. Puglisi.** 2002. NMR study of 100 kDa HCV IRES RNA using segmental isotope labeling. J. Am. Chem. Soc. **124:**9338–9339.
16. **Klinck, R., E. Westhof, S. Walker, M. Afshar, A. Collier, and F. Aboul-Ela.** 2000. A potential RNA drug target in the hepatitis C virus internal ribosomal entry site. RNA **6:**1423–1431.
17. **Krausslich, H. G., M. J. Nicklin, H. Toyoda, D. Etchison, and E. Wimmer.** 1987. Poliovirus proteinase 2A induces cleavage of eucaryotic initiation factor 4F polypeptide p220. J. Virol. **61:**2711–2718.
18. **Lemon, S. M., P. C. Murphy, P. A. Shields, L. H. Ping, S. M. Feinstone, T. Cromeans, and R. W. Jansen.** 1991. Antigenic and genetic variation in cytopathic hepatitis A virus variants arising during persistent infection: evidence for genetic recombination J. Virol. **65:**2056–2065.
19. **Low, W., M. Harries, H. Ye, M. Q. Du, C. Boshoff, and M. Collins.** 2001. Internal ribosome entry site regulates translation of Kaposi's sarcoma-associated herpesvirus FLICE inhibitory protein. J. Virol. **75:**2938–2945.
20. **Lukavsky, P. J., G. A. Otto, A. M. Lancaster, P. Sarnow, and J. D. Puglisi.** 2000. Structures of two RNA domains essential for hepatitis C virus internal ribosome entry site function. Nat. Struct. Biol. **7:**1105–1110.
21. **Ohlmann, T., M. Lopez-Lastra, and J. L. Darlix.** 2000. An internal ribosome entry segment promotes translation of the simian immunodeficiency virus genomic RNA. J. Biol. Chem. **275:**11899–11906.
22. **Ohlmann, T., M. Rau, V. M. Pain, and S. J. Morley.** 1996. The C-terminal domain of eukaryotic protein synthesis initiation factor (eIF) 4G is sufficient to support cap-independent translation in the absence of eIF4E. EMBO J. **15:**1371–1382.
23. **Pelletier, J., and N. Sonenberg.** 1988. Internal initiation of translation of eukaryotic mRNA directed by a sequence derived from poliovirus RNA. Nature **334:**320–325.
24. **Pestova, T. V., I. N. Shatsky, and C. U. Hellen.** 1996. Functional dissection of eukaryotic initiation factor 4F: the 4A subunit and the central domain of the 4G subunit are sufficient to mediate internal entry of 43S preinitiation complexes. Mol. Cell. Biol. **16:**6870–6878.
25. **Pilipenko, E. V., V. M. Blinov, B. K. Chernov, T. M. Dmitrieva, and V. I. Agol.** 1989. Conservation of the secondary structure elements of the 5′-untranslated region of cardio- and aphthovirus RNAs. Nucleic Acids Res. **17:**5701–5711.
26. **Ramos, R., and E. Martinez-Salas.** 1999. Long-range RNA interactions between structural domains of the aphthovirus internal ribosome entry site (IRES). RNA **10:**1374–1383.
27. **Reynolds, J. E., A. Kaminski, H. J. Kettinen, K. Grace, B. E. Clarke, A. R. Carroll, D. J. Rowlands, and R. J. Jackson.** 1995. Unique features of internal initiation of hepatitis C virus RNA translation. EMBO J. **14:**6010–6020.
28. **Rijnbrand, R., P. J. Bredenbeek, P. C. Haasnoot, J. S. Kieft, W. J. Spaan, and S. M. Lemon.** 2001. The influence of downstream protein-coding sequence on internal ribosome entry on hepatitis C virus and other flavivirus RNAs. RNA **7:**585–597.
29. **Rijnbrand, R., T. van der Straaten, P. A. van Rijn, W. J. Spaan, and P. J. Bredenbeek.** 1997. Internal entry of ribosomes is directed by the 5′ noncoding region of classical swine fever virus and is dependent on the presence of an RNA pseudoknot upstream of the initiation codon. J. Virol. **71:**451–457.
30. **Spahn, C. M., J. S. Kieft, R. A. Grassucci, P. A. Penczek, K. Zhou, J. A. Doudna, and J. Frank.** 2001. Hepatitis C virus IRES RNA-induced changes in the conformation of the 40s ribosomal subunit. Science **291:**1959–1962.
31. **Tsukiyama-Kohara, K., N. Iizuka, M. Kohara, and A. Nomoto.** 1992. Internal ribosome entry site within hepatitis C virus RNA. J. Virol. **66:**1476–1483.
32. **Vagner, S., A. Waysbort, M. Marenda, M. C. Gensac, F. Amalric, and A. C. Prats.** 1995. Alternative translation initiation of the Moloney murine leukemia virus mRNA controlled by internal ribosome entry involving the p57/PTB splicing factor. J. Biol. Chem. **270:**20376–20383.
33. **Wilson, J. E., M. J. Powell, S. E. Hoover, and P. Sarnow.** 2000. Naturally occurring dicistronic cricket paralysis virus RNA is regulated by two internal ribosome entry sites. Mol. Cell. Biol. **20:**4990–4999.